

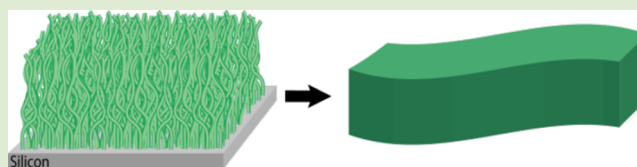
Characterization of Polymer Brush Membranes via HF Etch Liftoff Technique

M. Elizabeth Welch and Christopher K. Ober*

Departments of Chemistry and Chemical Biology and Material Science and Engineering, Cornell University, Ithaca, New York 14850, United States

S Supporting Information

ABSTRACT: Surface modification using end-tethered polymer brushes is an attractive, versatile, and effective method of tailoring the surface properties of a material. However, because the chains are covalently attached, characterization of these films is limited. When polymer brushes are detached in their native state, as opposed to fabricating a cross-linked initiator support, additional analytical techniques can be employed. We report lifting off patterned polymer brush membranes from a silicon oxide surface via a hydrofluoric acid etch. This method allows examination of polymer brushes via TEM and thus provides information regarding the perfection of initiator self-assembled monolayer formation and brush growth, as well as the effect of different cross-linking procedures.



In recent years, polymer brushes have garnered much attention because of their ability to alter surface properties on a scale of just a few nanometers. A surface can be modified with polymer brushes to create an interface compatible with biological environments.^{1,2} Such properties lead to applications in fields including bioelectronics, responsive surfaces, protein resistant surfaces, and biosensors.^{3–8}

Polymer brushes are polymer chains tethered to a surface or substrate. There are two common methods of attachment, “grafting from” and “grafting to”. The grafting to technique involves first polymerizing the chain and attaching an anchor group to the chain that can then bind to the surface. However, due to steric repulsion between incoming chains and chains already attached, the grafting density can be rather low. The grafting from method, on the other hand, can produce high density polymer brushes by first immobilizing an initiator molecule on the surface and subsequently growing chains through polymerization techniques such as atom transfer radical polymerization (ATRP), nitroxide-mediated polymerization (NMP), and reversible addition–fragmentation chain transfer (RAFT).^{9,10}

Because the chains are covalently attached to a substrate, characterization of the film may be difficult or provide an incomplete picture of the brush. Brushes are commonly characterized by water contact angle, IR/FTIR (chemical content), ellipsometry (thickness), and AFM (surface roughness). IR, contact angle, and ellipsometry measurements evaluate large areas and provide information about the brush averaging over this region. AFM instead looks at much smaller regions, but it is limited to surface characterization and provides little information about the subsurface of the brush film. None of these methods can give much insight into the effect of localized chain stretching or packing density of the brush regions. Much more information could be obtained if the brush were not bound to a surface. In order to characterize the film

itself, a polymer brush film removed from a surface enables additional types of detailed study. This new field of polymer brush analysis is just beginning to be explored. Amin et al. have prepared polymer carpets by depositing an electron-beam cross-linking self-assembled monolayer (SAM) of biphenyl on a support and subsequently growing polymer brushes from it through surface-initiated polymerization of vinyl monomers.¹¹ Then this layer was removed for analysis. Other researchers have expanded on this method of a cross-linked initiator surface and transferred polymer carpets to a graphene surface as a way of chemical functionalization.¹² Due to the biocompatibility of polymer brushes,¹³ applications in other fields such as biosensors and Janus membranes could be well suited for use of these polymer brush films.

We have developed a straightforward technique to remove patterned sections of polymer brushes, using polystyrene (PS) and poly(glycidyl methacrylate) (PGMA) brushes to test our approach. Both cross-linked and un-cross-linked polymer brushes (the latter as a control) were detached and subsequently analyzed by transmission electron microscopy (TEM). Our initial reasoning was that the polymer brushes should be cross-linked in order to retain physical integrity. The different cross-linking processes used were investigated to gain a better understanding of the resulting polymer brush membrane’s physical and chemical characteristics.

Previous work on polymer brush nanochannels led us to recognize the surprising strength of bridging brush layers stretched over distances ranging from 100 nm to a few micrometers.¹⁴ Therefore, we have developed a method of detaching polymer brush films that enables their further

Received: December 19, 2012

Accepted: February 6, 2013

Published: February 27, 2013

exploration (Figure 1). A 2 μm silicon oxide (SiO_2) layer thermally grown on a standard silicon wafer was selected for

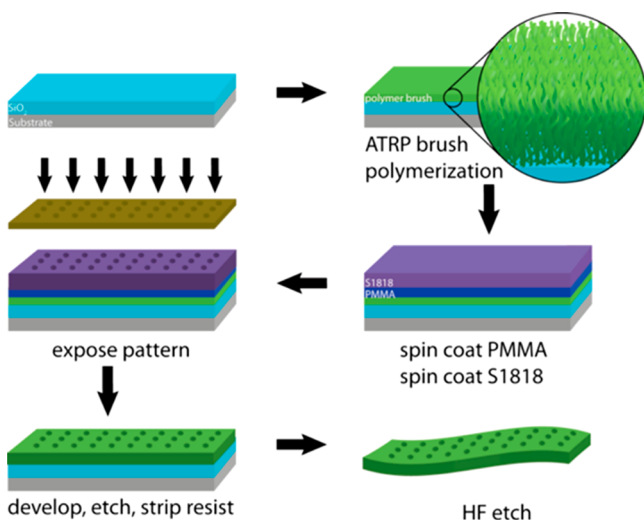


Figure 1. Detachment scheme producing membranes that can be transferred to TEM grids.

brush polymerization for two reasons. First, in terms of brush growth, it is chemically equivalent to the silicon wafer surface and thus initiator immobilization and brush polymerization environments will not affect or remove the oxide film. As a result, we are not limited to the type of polymer brushes that can be investigated with this technique. Second, SiO_2 can be dissolved by hydrofluoric (HF) acid. HF etches oxides but it does not harm polymers and therefore will not affect the polymer brush membranes. The brush films can then be rinsed repeatedly with water to remove HF and transferred to TEM grids for further characterization.

Instead of using a cross-linked SAM layer, as noted above, our method of detachment employs a HF acid etching process that preserves the initiator layer in its un-cross-linked state and allows for analysis of initiator immobilization uniformity (Figure 1). Results show initiator immobilized at low concentrations produces lower density, patchy brushes, whereas initiator immobilized at high concentrations generates high density, homogeneous brushes. This finding is in accordance with previous investigations regarding the mechanism of SAM formation.^{15,16}

They show that at room to low temperature, island domains will nucleate in the plane of the surface (Figure 2).^{17–20} Experimental parameters found to have a high impact on the mechanism included water content, deposition time, and temperature.^{17,21} We have determined that initiator concen-

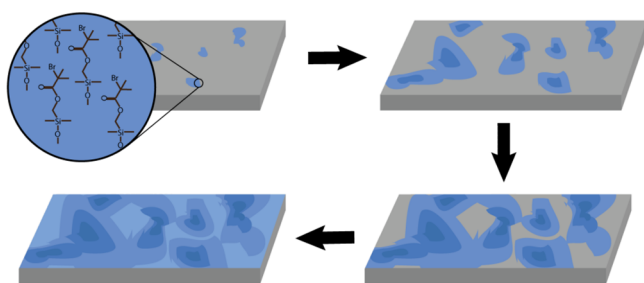


Figure 2. Initiator SAM formation via island mechanism.

tration also influences the quality of initiator layer formed and thus polymer brush film growth. Our method of membrane liftoff provides the opportunity to analyze initiator quality, immobilization conditions, and optimization parameters.

A first topic of study was the uniformity of the polymer brush layer. The quality of this layer is indicative of the homogeneity of the initiator immobilization step. As noted above, the SAM formation process involves assembly of islands prior to formation of a complete and uniform layer. Typical characterization of the SAM island formation includes AFM, optical ellipsometry, scanning tunneling microscopy (STM), and lateral force microscopy (LFM).^{22–24} However, SAMs of our ATRP initiator can also be characterized via analysis of the polymer brushes grown from them. The coverage density of polymer brushes is largely dependent on the quality of the initiator surface. A closely packed initiator surface allows for polymerization of high grafting density brushes. Therefore by examining the density of the polymer brushes, we can acquire information regarding our initiator deposition via TEM bright field mode. Previous studies have used AFM to distinguish buckling and folding; however it is extremely difficult to do AFM on detached films. TEM is important because we need a way to visualize detached membranes. This technique can probe fine detail and provide contrast information, which to a first approximation may be modeled by Beer's law. The enhanced sensitivity and additional contrast formation data provides clear indications of how dense our polymer brushes are and what regime we are working in (patchy brushes vs uniform brushes). It is important to establish growth conditions because, for example, when exploring the concept of brush stretching and expansion (discussed later) we only use the high density, uniform brush conditions.

Figure 3 shows TEM images of PS and PGMA membranes at different initiator concentrations. On average, we find initiator immobilization concentrations less than 2 mM generate "patchy" brushes. The brushes appear to be less dense in some areas and denser in others. We speculate this is because

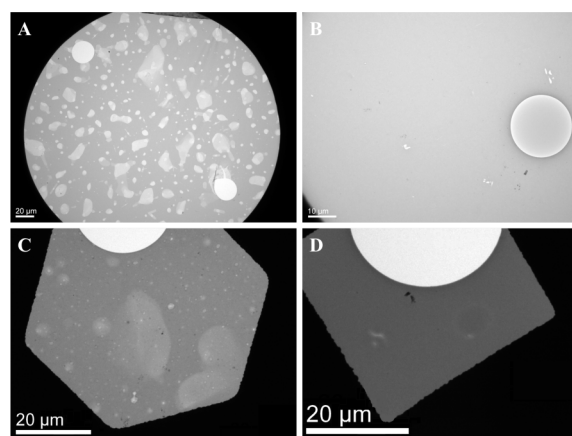


Figure 3. (A) TEM image of cross-linked PS brush membrane at 1 mM initiator immobilization concentration and (B) 20 mM: (A) shows a brush membrane with irregular thickness caused by heterogeneous deposition of initiator, while the higher concentration in (B) leads to a uniform brush membrane. (C) Un-cross-linked PGMA brush membrane at 1 mM and (D) 8 mM initiator immobilization concentration. As above, the lower concentration of initiator in (C) leads to brush thickness variations. See Supporting Information for analysis of heterogeneous brush.

our initiator immobilization follows the island formation mechanism where domains will nucleate and eventually grow together instead of proceeding by homogeneous deposition. At low initiator concentrations, complete coverage cannot be achieved. However, when the initiator concentration is increased, these irregular regions are no longer observed and instead a uniform membrane is produced. AFM results support these TEM findings. Figure 4 shows un-cross-linked PGMA

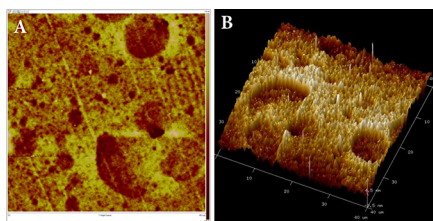


Figure 4. AFM of un-cross-linked PGMA film height image (a) and 3D image (b).

brush films removed from the substrate and allowed to settle back down on the surface for AFM characterization. Just as before, at low initiator immobilization concentrations we noticed patchy, irregular brushes. The height difference between these regions is 2–6 nm and confirms our TEM data observations.

Using imaging processing software, we were able to further analyze the patchy films and the approximate densities of the irregular regions. Based on previous reports,²⁵ the optical density (ϕ) of an area can be calculated from a ratio of the $\phi_{\text{hole}}/\phi_{\text{film}}$ (see Supporting Information). Numerous points of observation including the marker hole, homogeneous sections, and thin regions were selected and measured. For a PS film that was 76 nm thick in the dense brush region, the thin regions were shown to vary between 50 to as few as 10 nm. These films had breaks between the thick brush and thin regions, so measurements of surface properties would show the surface characteristics of polystyrene, even though the brush varied greatly from region to region. Calculations were carried out to give the relative thickness of the regions which, coupled with binary imagery processing, can provide overall area coverage. Analysis of the PS and PGMA TEM images using ImageJ (Figure 3a,c) shows the overall coverage by full thickness brushes to be $\sim 75\%$ in both cases, indicating the quality of the brush is determined by the initiator monolayer and not the nature of the monomer. This demonstration justifies the utility of this liftoff method as a means of better understanding the type of brush regime and coverage being produced. Moreover, it should be noted that this trend seems to be independent of polymer brush type and different polymerization environments. Thus, by lifting polymer brush films from a substrate and characterizing them via TEM, we can determine the quality and coverage of brushes our system is producing as well as the immobilization efficiency of our ATRP initiator.

Different polymer brush thicknesses have been explored with this technique ranging from 30 to 190 nm. Regardless of thickness, all films have proven to be surprisingly robust. Both cross-linked and un-cross-linked polymer brush membranes were preserved after detachment and had a tendency to fold, wrinkle, or buckle instead of tearing or fracturing. They also maintain their structure and composition under high vacuum in the TEM. This is consistent with our original study of polymer brush bridges spanning over nanochannel distances of a few

micrometers without collapse or breakage. Huck has also shown that it is possible to electrochemically detach brush films and that these brush layers remain intact.²⁶ These observations imply that such films can potentially undergo further functionalization and remain whole.

Further exploration of the effect of cross-linking polymer brushes before removal from the surface was investigated by both lithographic and chemical methods (Figure 5a). After the

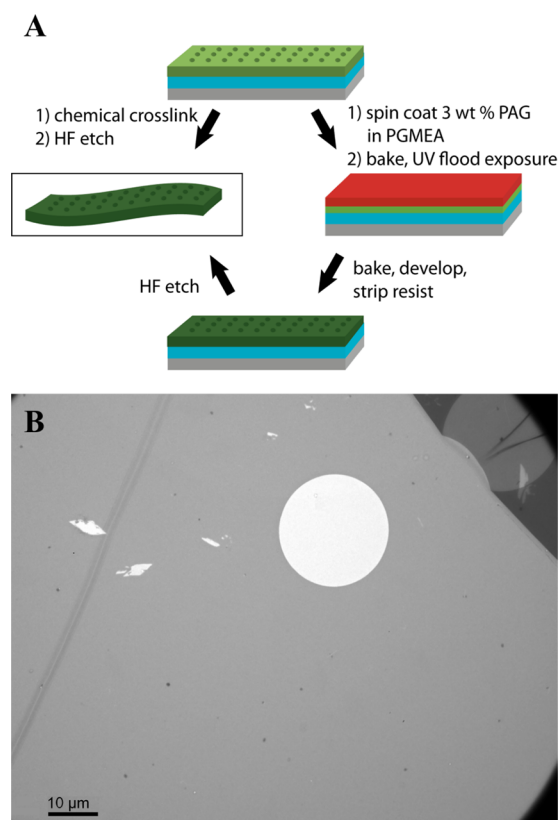


Figure 5. (A) Schematic of chemical and lithographic methods of cross-linking polymer brushes. (B) TEM image of UV cross-linked PS brush film. Figure shows uniform brush membrane with 20.94 μm patterned hole. In the upper right part of figure, the membrane has folded and an additional hole is observed. The center of the hole is two layers thick, while the darkest region is three layers thick. For analysis of this TEM, see Supporting Information.

polymer brushes were grown from the silicon oxide layer, they were patterned into individual membranes with holes 20 μm in diameter spaced 180 μm apart. These shapes and dimensions were chosen to serve as points of reference for TEM and optical microscopy, although other patterns and dimensions are possible as well. Results showed patterned holes of un-cross-linked membranes expanded to diameters of 30–32 μm , but if a cross-linking process was applied, the films retained shapes closer to that of the original 20 μm diameter pattern. We do not believe this expansion is due to the swelling of the polymer brushes. During our patterning and liftoff procedure, residual solvents are extracted, generating polymer brush membranes in the glassy state. The observation of change in dimension is then due to the chain relaxation from substrate release and not from swelling. Other studies have suggested stress relaxation associated with high surface packing and chain concentration (leading to Eigen strain) is a significant contributing factor to the mechanical properties of polymer brushes.²⁷ Such strain

drives the release process in both cross-linked and un-cross-linked films. To prevent this expansion, we have looked into various forms of cross-linking. Polystyrene is known to cross-link under prolonged exposure to UV radiation through UV-generated free radicals.^{28,29} To ensure full cross-linking, patterned PS samples were exposed to UV radiation for 10 min before the HF etch step. TEM images confirmed the original circles maintained their 20 μm diameter, thus, establishing that this method of cross-linking is successful for PS (Figure 5b).

Different techniques of cross-linking were explored for PGMA brushes. First, both acid and base reactions were tested using triflic acid, KOH, and ethylenediamine to cause cross-linking. FTIR of the strong acid and strong base cross-linking reactions was analyzed to verify the chemical change (see Supporting Information). Results showed an increased presence of absorption peaks consistent with the formation of ether bonds, thus, suggesting the epoxy ring opened up to form new linkages with neighboring chains. The same cross-linking effect is demonstrated via TEM characterization. Table 1

Table 1^a

cross-linking method	patterned hole diameter (μm)	hole diameter after liftoff (μm)	film expansion strain (%)
1 M KOH	20	20	0
1 M triflic acid	20	23	15
1 M ethylenediamine	20	27	35
photoacid generator	20	23	25

^aExpansion of hole diameter after liftoff was measured by TEM. Film expansion strain is the nominal strain or change in hole diameter relative to the starting dimension.

summarizes the results by examining the expansion of the patterned regions. As shown, more vigorous acids and bases are required to effectively cross-link the epoxide side groups; however, it should be noted that high concentration and long exposure times of these strong acids and bases can destroy the brush. Concentrations over 2 M and overnight reaction times lead to the polymer brushes being stripped from the surface and dissolved in solution. Lower concentrations (1 M) and reaction times under 2 h lead to polymer brush cross-linking without damage. In addition to chemical cross-linking, lithographic techniques can also be employed. Introducing a photoacid generator (PAG) and using UV radiation is a promising method. Typical PAGs are compounds added to a spin coating solution that decompose upon exposure to yield free radicals or cations. A standard PAG (1–3 wt %) was added to PGMEA solvent and spin coated directly on the polymer brushes. The substrate was then exposed to UV radiation for 1.5 min, baked, and developed. The generated strong acid can diffuse into the brushes, open the epoxy rings, and cross-link the brushes similar to triflic acid. As shown in Table 1, both the triflic acid and PAG approaches produce similar cross-linking results. By lifting the polymer brush membranes from the surface and analyzing the expansion of the patterned features, the efficiency of various cross-linking techniques can be investigated.

We have developed a method of removing polymer brush membranes from a surface for detailed characterization. Polymerizing polymer brushes via ATRP from silicon oxide and employing an HF etch to lift off the film allows numerous

types of brushes to be analyzed. Because silicon oxide is chemically stable in organic solvents, we are not limited to a particular type of brush. Additionally, HF only etches oxides; hence, the polymer membranes are not chemically sacrificed. Analysis by TEM provides more information about the initiator immobilization and brush polymerization process. At low initiator immobilization concentrations, polymerization leads to patchy brushes comprised of isolated areas of decreased brush density. We believe this observation is indicative of the island formation mechanism for SAMs in general and this method can provide insight into polymer brush initiator immobilization parameters and the types of brushes that can be produced. Heterogeneous brush formation takes place under conditions that have been reported in the literature that are assumed to form uniform brush layers. AFM is unlikely to reveal this irregularity unless this is being specifically looked for.

As we expected, cross-linked brushes can be removed from the Si substrate to produce robust polymer films that retain the original patterned dimension. By first patterning the polymer brushes, we establish reference points from which to base our findings after membrane liftoff. Patterned circles of a specific diameter were examined before and after film removal and brush film size was analyzed to confirm the effectiveness of different cross-linking processes. Surprisingly when un-cross-linked brush layers are removed, they remain intact and expand in the x-y plan due to chain relaxation caused by Eigen strain release first introduced during the original brush growth process. Overall, this polymer brush film removal system can provide information regarding initiator immobilization, brush polymerization/functionalization methods, and answer questions about the nature of these brush films.

■ ASSOCIATED CONTENT

📄 Supporting Information

Synthesis of the ATRP silane initiator, polymerization of both PS and PGMA brushes, patterning and etch, cross-linking methods, and TEM characterization of the brushes. This material is available free of charge via the Internet at <http://pubs.acs.org>.

■ AUTHOR INFORMATION

✉ Corresponding Author

*E-mail: cko3@cornell.edu.

Notes

The authors declare no competing financial interest.

■ ACKNOWLEDGMENTS

The authors would like to acknowledge the National Science Foundation Grant DMR-1105253 for support of this work. This work made use of the Cornell Center for Materials Research Shared Facilities which are supported through the NSF MRSEC program (DMR-1120296), the Nanobiotechnology Center shared research facilities at Cornell University, and was performed in part at the Cornell NanoScale Facility, a member of the National Nanotechnology Infrastructure Network, which is supported by the NSF (Grant ECS-0335765).

■ REFERENCES

- (1) Jancar, J.; Douglas, J. F.; Starr, F. W.; Kumar, S. K.; Cassagnau, P.; Lesser, A. J.; Sternstein, S. S.; Buehler, M. J. *Polymer* **2010**, *51*, 3321–3343.

- (2) Yuan, J. Y.; Xu, Y. Y.; Muller, A. H. E. *Chem. Soc. Rev.* **2011**, *40*, 640–655.
- (3) Welch, M.; Rastogi, A.; Ober, C. *Soft Matter* **2011**, *7*, 297–302.
- (4) He, H. T.; Jing, W. H.; Xing, W. H.; Fan, Y. Q. *Appl. Surf. Sci.* **2011**, *258*, 1038–1044.
- (5) Ionov, L.; Minko, S. *ACS Appl. Mater. Int.* **2012**, *4*, 483–489.
- (6) Rodriguez-Emmenegger, C.; Brynda, E.; Riedel, T.; Houska, M.; Subr, V.; Alles, A. B.; Hasan, E.; Gautrot, J. E.; Huck, W. T. S. *Macromol. Rapid Commun.* **2011**, *32*, 952–957.
- (7) Tria, M. C. R.; Grande, C. D. T.; Ponnampati, R. R.; Advincula, R. C. *Biomacromolecules* **2010**, *11*, 3422–3431.
- (8) Zhu, L.; Zhao, B. J. *Phys. Chem. B* **2008**, *112*, 11529–11536.
- (9) Edmondson, S.; Osborne, V. L.; Huck, W. T. S. *Chem. Soc. Rev.* **2004**, *33*, 14–22.
- (10) Pyun, J.; Kowalewski, T.; Matyjaszewski, K. *Macromol. Rapid Commun.* **2003**, *24*, 1043–1059.
- (11) Amin, I.; Steenackers, M.; Zhang, N.; Beyer, A.; Zhang, X. H.; Pirzer, T.; Hugel, T.; Jordan, R.; Golzhauser, A. *Small* **2010**, *6*, 1623–1630.
- (12) Steenackers, M.; Gigler, A. M.; Zhang, N.; Deubel, F.; Seifert, M.; Hess, L. H.; Lim, C.; Loh, K. P.; Garrido, J. A.; Jordan, R.; Stutzmann, M.; Sharp, I. D. *J. Am. Chem. Soc.* **2011**, *133*, 10490–10498.
- (13) Andruzzi, L.; Senaratne, W.; Hexemer, A.; Sheets, E. D.; Ilic, B.; Kramer, E. J.; Baird, B.; Ober, C. K. *Langmuir* **2005**, *21*, 2495–2504.
- (14) Paik, M. Y.; Xu, Y. Y.; Rastogi, A.; Tanaka, M.; Yi, Y.; Ober, C. K. *Nano Lett.* **2010**, *10*, 3873–3879.
- (15) Schreiber, F. *Prog. Surf. Sci.* **2000**, *65*, 151–256.
- (16) Onclin, S.; Ravoo, B. J.; Reinhoudt, D. N. *Angew. Chem., Int. Ed.* **2005**, *44*, 6282–6304.
- (17) Bierbaum, K.; Grunze, M.; Baski, A. A.; Chi, L. F.; Schrepp, W.; Fuchs, H. *Langmuir* **1995**, *11*, 2143–2150.
- (18) Brzoska, J. B.; Benazouz, I.; Rondelez, F. *Langmuir* **1994**, *10*, 4367–4373.
- (19) Parikh, A. N.; Allara, D. L.; Azouz, I. B.; Rondelez, F. *J. Phys. Chem.* **1994**, *98*, 7577–7590.
- (20) Brzoska, J. B.; Shahidzadeh, N.; Rondelez, F. *Nature* **1992**, *360*, 719–721.
- (21) Reiniger, M.; Basnar, B.; Friedbacher, G.; Schleberger, M. *Surf. Interface Anal.* **2002**, *33*, 85–88.
- (22) Stranick, S. J.; Parikh, A. N.; Tao, Y. T.; Allara, D. L.; Weiss, P. S. *J. Phys. Chem.* **1994**, *98*, 7636–7646.
- (23) Liu, Y.; Wolf, L. K.; Messmer, M. C. *Langmuir* **2001**, *17*, 4329–4335.
- (24) Dinh, D. H.; Vellutini, L.; Bennetau, B.; Dejous, C.; Rebiere, D.; Pascal, E.; Moynet, D.; Belin, C.; Desbat, B.; Labrugere, C.; Pillot, J. P. *Langmuir* **2009**, *25*, 5526–5535.
- (25) Lauterwasser, B. D.; Kramer, E. J. *Philos. Mag. A* **1979**, *39*, 469–495.
- (26) Edmondson, S.; Frieda, K.; Comrie, J. E.; Onck, P. R.; Huck, W. T. S. *Adv. Mater.* **2006**, *18*, 724–728.
- (27) Annabattula, R. K.; Huck, W. T. S.; Onck, P. R. *J. Mech. Phys. Solids* **2010**, *58*, 447–465.
- (28) Knudsen, D.; Harnish, B.; Toth, R.; Yan, M. D. *Polym. Eng. Sci.* **2009**, *49*, 945–948.
- (29) Mu, B.; Shen, R. P.; Liu, P. *Nanoscale Res. Lett.* **2009**, *4*, 773–777.